Efficient modelling of flexible cable-pulley systems

Markus Spiegelhauer[1] · Berthold Schlecht[1]

Abstract

This article proposes a universal procedure for efficiently modelling the flexible behaviour of pre-stressed cables, guided by multiple pulleys. Such cable-pulley systems usually connect various structural components, which often feature additional flexibility. One concern in holistic system analyses is to correctly describe the elasticity of the entire assembly for one particular spatial configuration. This can be achieved in terms of a linear stiffness matrix that accounts for the kinematics of the assembly. In this article, parametric stiffness matrices for arbitrary cable-pulley arrangements are derived. A reduction scheme is used to facilitate the integration of the derived stiffness matrix into superordinate finite element models. The method is validated with a non-linear finite element model and applied to a complex hoisting cable system connecting multiple large steel structures.

Effiziente Modellierung elastischer Seilzugsysteme

Zusammenfassung

Durch die Führung eines Seiles über mehrere Umlenkrollen lassen sich überaus vielseitig einsetzbare Mechanismen konzipieren. Die Kinematik eines derartigen Seilzugsystems erlaubt die Bewegung großer Lasten mit geringem Krafteinsatz. Wird das Seil jedoch als elastisch angenommen, ergeben sich komplexe Zusammenhänge für die effektive Steifigkeit zwischen den Anbindungspunkten des Seilsystems an die umgebende Struktur.

Der vorliegende Beitrag stellt ein allgemeingültiges Modellierungsverfahren vor, das die Abbildung der Elastizität axial belasteter Seilzugsysteme mit mehreren Umlenkrollen gestattet. Grundlage hierfür bildet die Ableitung der Steifigkeitsmatrix eines Seilsystems mit beliebig angeordneten Seilabschnitten und Umlenkrollen. Um die Einbindung der parametrischen Steifigkeitsmatrix des Seilsystems in übergeordnete Finite-Elemente-Modelle zu erleichtern, wird ein Ansatz zur Freiheitsgradreduktion angewendet. Das vorgestellte Verfahren wird zunächst für die Modellierung eines einfachen Flaschenzuges genutzt. Am selben Minimalmodell erfolgt die Validierung der Methode mittels eines nichtlinearen Finite-Elemente-Modelles. Die Anwendbarkeit bei Mechanismen größerer Komplexität wird anhand der Modellierung eines Hubseilsystems demonstriert, das über Dutzende Anbindungspunkte mehrere Stahlbaustrukturen koppelt. Der Einfluss der Seilsystemmodellierung auf das niederfrequente Schwingungsverhalten des Gesamtsystems wird simulativ untersucht und mit Messdaten verglichen.

1 Introduction

Cables, especially those made from twisted or braided steel wire and referred to as wire rope, are basic mechanical elements of great significance in material handling tech-nology. The individual steel wires of high tensile strength are mainly subjected to axial loads. As a result, even wire ropes with small cross-sectional areas – and thus low dead weight – offer a high load-bearing capacity. *Stationary ropes* that are firmly clamped at two remote points allow to guy structural components. Due to the cable's bending flexibility, sheaves can be used to deflect it, leading to *running ropes* [1]. If multiple sheaves are arranged, robust and yet compact mechanisms arise, which both change the direction and the magnitude of forces. The mechanical advantage of those cable-pulley systems justifies the uti-

✉ Markus Spiegelhauer
markus.spiegelhauer@tu-dresden.de

1 Institute of Machine Elements and Machine Design (IMM),
TU Dresden, Münchner Platz 1–3, 01187 Dresden, Germany

lization of smaller drives and cables of reduced diameter. Typical fields of application are elevators, mobile and tower cranes, the running rigging of sailing ships and hoisting gear in general.

Cables experience a longitudinal elongation caused by loads in operating conditions. The corresponding stiffness of a single stationary cable can be calculated according to Ref. [2] based on its geometrical properties and the wire's material.[1] Systems comprising of pulleys and several cable segments, and connecting multiple points exhibit a less obvious behaviour: The sheave's rotational degree of freedom allows the cable to pass and therefore causes a change in tension within both connected cable segments. Under external loading, the tensile forces in all cable segments balance. Consequently, the stiffness between arbitrary points of the cable system is no longer exclusively depending on the stiffness of the individual segments.

The elastic interdependence of all attachment points of a cable-pulley system is of particular interest for various cases:

- Static analyses considering the deformation of the overall system
- Sub-system analyses requiring the loads at the interfaces
- Time-domain simulations of large dynamic systems
- Holistic frequency-domain modelling of elastic structures targeting active vibration control and dynamic optimization

The theory of wire rope regarding the deformation behaviour and the strength under various loading conditions has been covered in depth [2, 3]. Numerous contributions [4–9] are dedicated to spatially discretized models of cables for non-linear static and dynamic finite element and multibody simulations. A common approach is the modelling of cables as a series of elastic links, connected by spherical joints [4, 5]. To simulate the curvature of cables without pre-tension or even under compression, special high order non-linear finite elements [7, 8] have been proposed. If cables modelled by means of finite elements are undergoing large deflection in multi-body simulations, the absolute nodal coordinate formulation (ANCF) provides a suitable method to include the non-linear dynamical behaviour. [9] Common to all these models is the large number of additional degrees of freedom that is introduced for every cable segment.

The study [10] explicitly deals with a cable passing through a single pulley. A three-node finite element is presented and applied to the analysis of transmission line cables. Formulations suitable for cable-pulley assemblies that connect multiple nodes have been developed [11–13]. The authors introduce an additional degree of freedom per pulley which is denoted as "cable passage". Since the resulting stiffness matrix also has these additional degrees of freedom, integration into superordinate finite element models is made more complicated. Fields of application for the proposed approach are the static analysis of a spreader bar [11] and computer animations of a tower crane [12].

This article proposes a universal procedure for efficiently modelling the flexible behaviour of pre-stressed cable-pulley systems. A cable-system model derived using the introduced method allows to couple multiple compliant structural components in holistic simulations, focussing on the static and lower frequency dynamic behaviour of the entire system. The method relies on several assumptions:

- One equilibrium configuration of the system is analysed. The cable length is assumed to remain constant.
- The cable mass can be neglected compared to the inertia of the connected structural components or the attached lifting mass.
- Transversal vibrations of the cable itself do not affect the dynamics of the overall system.

First, variational principles are utilized to derive parametric stiffness matrices for cable-pulley arrangements in general, taking into account the kinematics of the assembly. The initially introduced coordinates, which describe the sheaves' rotations, are eliminated by means of a reduction scheme, leading to a reduced order stiffness matrix. As this reduced matrix does only contain the translational degrees of freedom associated with the attachment points, integration in finite element software is facilitated.

The approach is then applied to a simple block and tackle and validated with a detailed finite element model including contact. It is shown that an oversimplified model, which completely neglects the rotations of the sheaves, leads to physically implausible results. Hereafter, the procedure is applied to a complex cable-pulley arrangement connecting multiple large steel structures of a bucket wheel excavator. The effect of the proposed modelling approach on the low-frequency vibration characteristics of an overall finite element model of the excavator's superstructure is analysed and compared with measured data of the real system. As the presented holistic simulation model sufficiently describes the dynamics in the frequency range of interest, control strategies for the active suppression of unwanted vibrations during normal operation can be analysed and evaluated in future work.

---

[1] In general, the stress-strain relationship of wire ropes is non-linear. Nevertheless, one defines an effective modulus of elasticity, which relates stress and strain and depends on the present tension [2].

2 Method

Starting with Lagrange's equations of a conservative system, the dynamics of the system can be expressed in terms of n generalized coordinates q_i as

$$\frac{d}{dt}\left(\frac{\partial T}{\partial q_i}\right) - \frac{\partial T}{\partial q_i} + \frac{\partial V}{\partial q_i} = 0, \quad \text{with } i = 1 \dots n, \tag{1}$$

were T and V denote the kinetic and potential energy, respectively. Let $\vec{q} = \vec{0}$ describe an equilibrium configuration of the system. A multi-variable Taylor series expansion of the potential V around this equilibrium yields [14]

$$\begin{aligned} V(\vec{q}) = V(\vec{0}) &+ \sum_{i=1}^{n}\left(\frac{\partial V}{\partial q_i}\right)_{\vec{q}=\vec{0}} \cdot q_i \\ &+ \frac{1}{2}\sum_{i=1}^{n}\sum_{j=1}^{n}\left(\frac{\partial^2 V}{\partial q_i \partial q_j}\right)_{\vec{q}=\vec{0}} \cdot q_i q_j + \mathcal{O}(\vec{q}^3). \end{aligned} \tag{2}$$

As the expansion is carried out in the neighbourhood of the equilibrium position, the term $(\partial V/\partial q_i)_{\vec{q}=\vec{0}}$ vanishes, since by definition $\vec{q} = \vec{0}$ is a local minimum of $V(\vec{q})$. If the goal is to describe the system's behaviour due to small disturbances (e.g. vibrations) the Taylor series may be truncated after the quadratic term. The absolute value of the potential $V(\vec{0})$ does not affect the system's behaviour in the vicinity of the equilibrium. Consequently, the potential, may be expressed as a second order approximation

$$V(\vec{q}) \propto \frac{1}{2}\sum_{i=1}^{n}\sum_{j=1}^{n} k_{ij} \cdot q_i q_j = \frac{1}{2}\vec{q}^T \mathbf{K} \vec{q}. \tag{3}$$

The right term represents the potential energy in matrix-vector form. This introduces the *linear* stiffness matrix $\mathbf{K}$, which is symmetric and positive definite [14]. Its coefficients are obtained by comparison with Eq. (2)

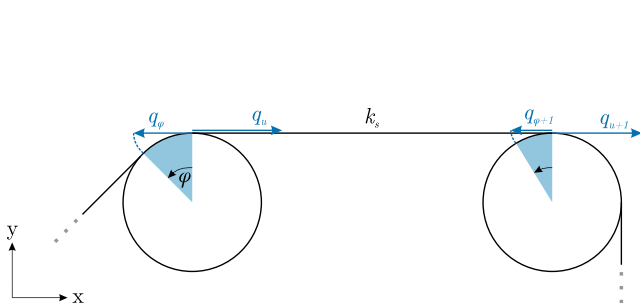$$k_{ij} = \frac{\partial^2 V}{\partial q_i \partial q_j}. \tag{4}$$

Therefore, the stiffness matrix of the entire system is calculated according to this strictly formal procedure based on one scalar quantity V.

The system's overall potential energy is formed by the energies of the individual cable portions, which need to be expressed as a function of the generalized coordinates. Fig. 1 depicts one horizontally aligned cable segment s, guided by two pulleys. Both horizontal displacements q_u and q_{u+1} of the pulleys' axles can cause an elastic deformation of the cable section. The translation of a pulley may either arise from deformations of the supporting structure or from rigid body motion of the attachment point. In addition, the coordinates q_φ and $q_{\varphi+1}$ are introduced, describing the arc length of the cable passing due to the pulleys' rotations. This permits to formulate the potential energy in relation to the effective change in length and the nominal stiffness k_s

$$V_s = \frac{1}{2}k_s(\underbrace{-q_u + q_{u+1}}_{\text{pulley disp.}} + \underbrace{q_\varphi - q_{\varphi+1}}_{\text{cable motion}})^2. \tag{5}$$

One sheave is associated only with a single coordinate q_φ, even if two cable segments are attached. As a consequence, adjacent cable segments are coupled via these coordinates.

The general case of a cable segment with arbitrary spatial orientation $\vec{r}$ is shown in Fig. 2. Now the displacements of both pulleys are described by vectors $_A\vec{q}$ and $_B\vec{q}$. Only displacement components in the longitudinal direction of the cable affect its potential energy. Thus, an orthogonal projection of the displacement vector onto the cable is carried out, leading to

$$\begin{aligned} V_s = \frac{1}{2}k_s\left(-_A\vec{q}^T\vec{r} + q_\varphi + {_B\vec{q}}^T\vec{r} - q_{\varphi+1}\right)^2, \\ \text{where } ||\vec{r}||_2 = 1. \end{aligned} \tag{6}$$

The axial stiffness k_s of each cable segment in Eqs. (5) and (6) depends on its free length. As the position of pulleys

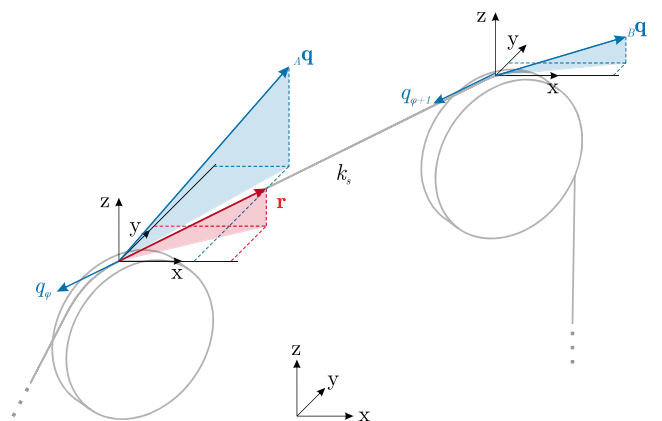**Fig. 1** Horizontally aligned cable segment with generalized coordinates

Fig. 2 Cable segment connecting two pulleys with arbitrary spatial orientation

can in general change considerably during hoisting, also the cable length in between – and thus the segment stiffness – will vary. A stiffness matrix of the cable system would be non-linear. It should be noted that the procedure described by Eq. (3) relies on the analysis of one spatial configuration of the cable system. In this case the cable segments have a defined length and fixed nominal stiffness, allowing to describe the flexible behaviour in terms of a linear stiffness matrix.

A stiffness matrix derived according to the presented method couples coordinates, which describe the displacements of attachment points as well as the pulleys' rotations. According to that, the vector of generalized coordinates is subdivided into $\vec{q}_u$, associated with the spatial movement of the pulley axles and $\vec{q}_\varphi$, representing the cable motion due to the pulley rotations. This enables to partition the stiffness matrix, yielding

$$\begin{bmatrix} \mathbf{K}_{uu} & \mathbf{K}_{u\varphi} \\ \mathbf{K}_{\varphi u} & \mathbf{K}_{\varphi\varphi} \end{bmatrix} \cdot \begin{bmatrix} \vec{q}_u \\ \vec{q}_\varphi \end{bmatrix} = \begin{bmatrix} \vec{f}_u \\ \vec{f}_\varphi \end{bmatrix} \tag{7}$$

as a relation between external loads $\vec{f}$ and displacements. If no loads (e.g. driving forces or friction) act on the coordinates related to the rotations of the pulleys $\vec{f}_\varphi = \vec{0}$ holds true. Therefore

$$\mathbf{K}_{\varphi u}\vec{q}_u + \mathbf{K}_{\varphi\varphi}\vec{q}_\varphi = \vec{0}. \tag{8}$$

may be rearranged in a way

$$\vec{q}_\varphi = -\mathbf{K}_{\varphi\varphi}^{-1}\mathbf{K}_{\varphi u}\vec{q}_u, \tag{9}$$

which allows to directly calculate the motion $\vec{q}_\varphi$ that balances cable tensions for a given displacement configuration $\vec{q}_u$. This enables to substitute $\vec{q}_\varphi$ in

$$\mathbf{K}_{uu}\vec{q}_u + \mathbf{K}_{u\varphi}\vec{q}_\varphi = \vec{f}_u, \tag{10}$$

finally leading to the reduced stiffness matrix $\mathbf{K}_{\text{red}}$ of a general cable-pulley assembly

$$\left(\mathbf{K}_{uu} - \mathbf{K}_{u\varphi}\mathbf{K}_{\varphi\varphi}^{-1}\mathbf{K}_{\varphi u}\right)\vec{q}_u = \mathbf{K}_{\text{red}}\vec{q}_u = \vec{f}_u. \tag{11}$$

The coupling between the displacement coordinates of all attachment points thus takes into account the cable passages, without explicitly introducing the respective degrees of freedom. Formally, this procedure is equivalent to the reduction scheme presented by Guyan [15]. As only additional relations between the already existing nodal degrees of freedom of a superstructure are introduced by the modelling approach, integration in finite element models – for example via user-defined superelements – is easily achieved.

3 Validation

The simple rope and tackle shown in Fig. 3 serves to demonstrate the approach and validate its results by means of a non-linear finite element model. The cable system's stiffness model and the finite element model will be compared in terms of natural frequencies and mode shapes of the specific spatial configuration displayed in Fig. 3.

The cable is assumed to be flexible in longitudinal direction. In contrast, the mounting points of the cable and the upper pulley are ideally rigid. A primary point mass is attached to a travelling block, whereas a second mass connects to the cable's free end. The system possesses a mechanical advantage of two. If both point masses have only one translational degree of freedom in vertical direction, four generalized coordinates are sufficient to describe the dynamics of the cable system.

According to Eq. (5) the potential energies of the rope sections could be derived as

$$\begin{aligned} V_1 &= \frac{k_1}{2}(-q_1 + q_3)^2 \\ V_2 &= \frac{k_2}{2}(q_1 + q_3 + q_4)^2 \\ V_3 &= \frac{k_3}{2}(-q_2 + q_4)^2 \end{aligned} \tag{12}$$

leading to the partitioned yet unreduced stiffness matrix

$$\mathbf{K} = \left[\begin{array}{c|c} \mathbf{K}_{uu} & \mathbf{K}_{u\varphi} \\ \hline \mathbf{K}_{\varphi u} & \mathbf{K}_{\varphi\varphi} \end{array}\right] = \left[\begin{array}{cc|cc} k_1+k_2 & 0 & k_2-k_1 & k_2 \\ 0 & k_3 & 0 & -k_3 \\ \hline k_2-k_1 & 0 & k_1+k_2 & k_2 \\ k_2 & -k_3 & k_2 & k_2+k_3 \end{array}\right]$$

that relates two translational coordinates $q_{1/2}$ to the cable motion expressed as $q_{3/4}$. The stiffness of each cable segment is determined based on its current length at the equilibrium configuration under investigation (see Fig. 3). With stiffness values of $k_1 = k_2 = 2k_3 = 2k$ and after eliminating $q_{3/4}$ using Eq. (11), one obtains the reduced stiffness matrix

$$\mathbf{K}_{\text{red}} = \begin{bmatrix} 2k & k \\ k & k/2 \end{bmatrix}. \tag{14}$$

The coefficient k_{22} can be used as a simple means of verifying the matrix. If q_1 is fixed, k_{22} describes the reaction force at the free end of the cable caused by a unit displacement on q_2. Therefore, k_{22} should equal the overall stiffness of the cable consisting of the three segments connected in series.

Fig. 3 Scheme of a block and tackle used to validate the approach (*left*). Modelling details of the finite element model (*right*)
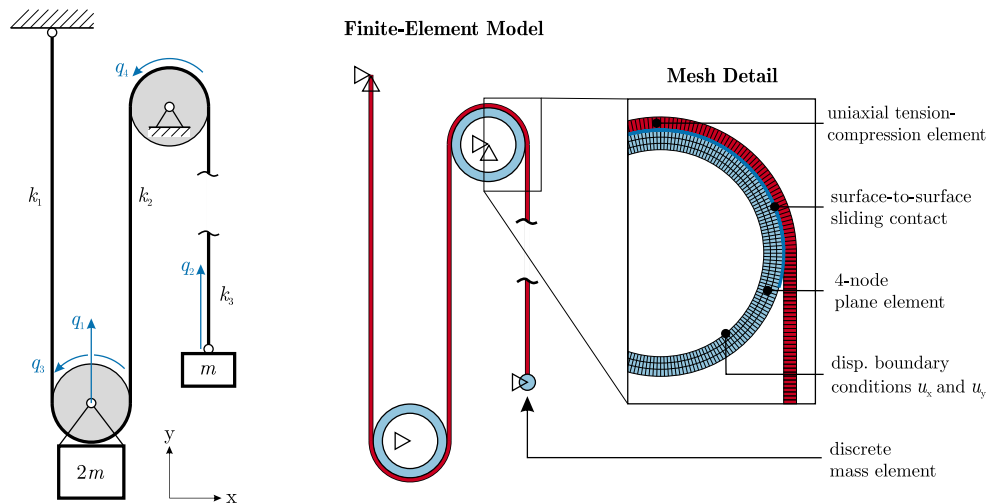
Since the sheaves and the cable itself are assumed to have a negligible inertia compared to the attached masses, the corresponding mass matrix is[2]

$$\mathbf{M}_{\text{red}} = \text{diag}\,(2m, m)\,. \tag{15}$$

To validate the modelling approach an undamped modal analysis of both the proposed analytical model and a detailed finite element model is carried out. The generalized eigenvalue problem $\left(\mathbf{K}_{\text{red}} - \omega^2 \mathbf{M}_{\text{red}}\right) \vec{\phi} = \vec{0}$ of the analytic cable stiffness model – with mass and stiffness matrices defined by eqs. 15 and 14 respectively – can be solved by hand. This provides the natural frequency matrix $\mathbf{\Lambda}$ and the mode shape matrix $\mathbf{\Phi}$

$$\mathbf{\Lambda} = \text{diag}\left(0, \frac{3k}{2m}\right) \qquad \mathbf{\Phi} = \begin{bmatrix} -0.5 & 1 \\ 1 & 1 \end{bmatrix} \tag{16}$$

The zero eigenvalue corresponds to a rigid body vibration mode, representing the lifting kinematics of a block and tackle. The only non-zero eigenvalue corresponds to an elastic normal mode, where both attached masses perform an in-phase motion.

Fig. 3 depicts the element types and the boundary conditions of the detailed finite element model, that was created in Ansys Mechanical. To ensure comparability with the derived cable stiffness model, the pulleys possess no rotational degree of freedom, cancelling their rotary inertia. In order to include the cable motion two frictionless surface-surface contacts between the cable and both pulleys have been set up. As the cable-pulley interaction is modelled using a sliding contact formulation, a fine discretization of the contact region – and therefore a large number of elements – is necessary. The contact exhibits a non-linear behaviour, requiring the linearization of the model prior to numerically solving the eigenvalue problem. Hence an operational load is applied on both masses in a first load step. After iteratively calculating an equilibrium state under the operational load, the system can be linearised using Ansys' linear perturbation procedure. The cable nodes remain free to slide tangentially, however the contact state is not allowed to change anymore. Subsequently, a prestressed modal analysis of the now linearised model can be carried out. Table 1 contrasts the results of a the proposed stiffness-based modelling approach with those of the detailed finite

Table 1 Different modelling approaches of increasing complexity and their comparison via modal parameters

Level of detail	ω_1^2 [s^{-2}]	ω_2^2 [s^{-2}]	$\vec{\phi}_1$	$\vec{\phi}_2$
Point-to-point stiffness	100.000	200.000	$[0.000\ 1.000]^T$	$[1.000\ 0.000]^T$
Cable stiffness model	0.000	150.000	$[-0.500\ 1.000]^T$	$[1.000\ 1.000]^T$
Finite element model	0.097	149.981	$[-0.499\ 1.000]^T$	$[1.001\ 1.000]^T$

---

[2] This assumption is usually valid for large-scale supporting structures, when only lower natural frequencies are of interest. If the inertia of the pulleys should be considered, an approximate reduction of the mass matrix according to Ref. [15] can be performed.
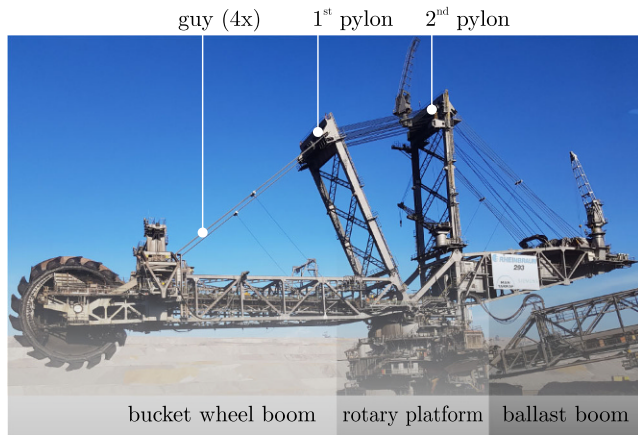
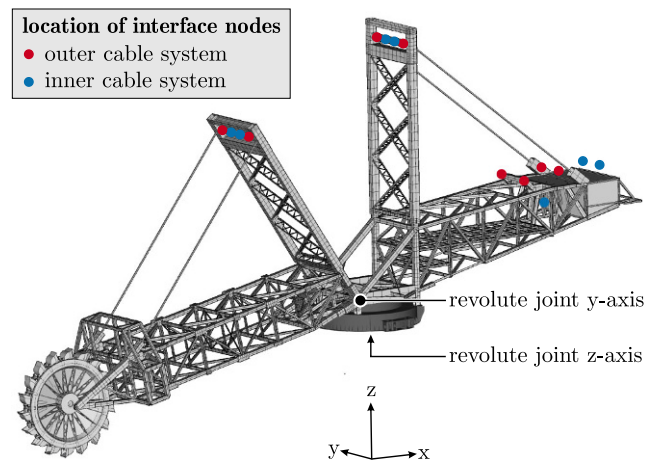Fig. 4 Bucket wheel excavator and its main components

Fig. 5 Topology of the finite element model

element model and an oversimplified point-to-point coupling approach. The numerical values for the stiffness and the mass were defined as $k = 1\,\text{N/m}$ and $m = 1 \cdot 10^{-2}\,\text{kg}$, respectively.

If the stiffness of individual cable segments is directly used to couple coordinates of adjacent pulleys (viz. only $\mathbf{K}_{uu}$ of Eq. (13) is accounted for), erroneous results arise. The mode shapes of this point-to-point stiffness approach reveal the absence of coupling between the two translational coordinates due to the neglected cable motion.

The results of the presented stiffness-based modelling method show good agreement with the finite element model, proofing the method's validity. Due to the absence of contact formulations and the reduced number of coordinates to solve, the computational expense decreases to only a fraction.

4 Application to a complex cable system

A more intricate system, which serves to demonstrate the proposed modelling approach is the large-scale open-cast mining equipment shown in Fig. 4. Two wide-span steel structures, the bucket wheel boom and the ballast boom equipped with a counterweight, are mounted on a rotary platform.

Crucial for the excavator's operation is the ability to change the inclination of the bucket wheel boom and therefore vary the mining height. This functionality is realized by means of two redundant hoisting cable systems, routed via pylons and allowing to change the distance between the upper ends of both pylons. As a pair of guy ropes links the first pylon and the bucket wheel boom, any change in length of the hoisting cable affects the position of the triangle formed by bucket wheel boom, first pylon and guy rope. Obviously, the hoisting cable systems directly influence the kinematics of the entire superstructure. Additionally, the cable stiffness contributes to the overall flexibility of the assembly and its vibration behaviour.

Table 2 Relevant vibration modes of the excavator's superstructure with the proposed cable system model and an oversimplified point-to-point coupling approach

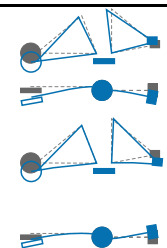| Mode number	Natural frequency [Hz]			Description of the mode shape	
	Measurement	Cable system model	Point-to-point approach		
1	0.33 ... 0.37	0.36	0.43	In-phase pitching	
2	0.64 ... 0.66	0.67	0.73	Horizontal deflection	
3	0.97 ... 1.00	1.00	1.35	Out-of-phase pitching	
4	not excited	1.08	1.08	Torsion of bucket wheel boom	
5	1.16 ... 1.18	1.14	1.33	Horizontal deflection	
6	1.21 ... 1.23	1.21	1.48	Torsion of both booms	

Fig. 6 Complex cable-pulley system used to hoist the bucket wheel boom of a large-scale excavator
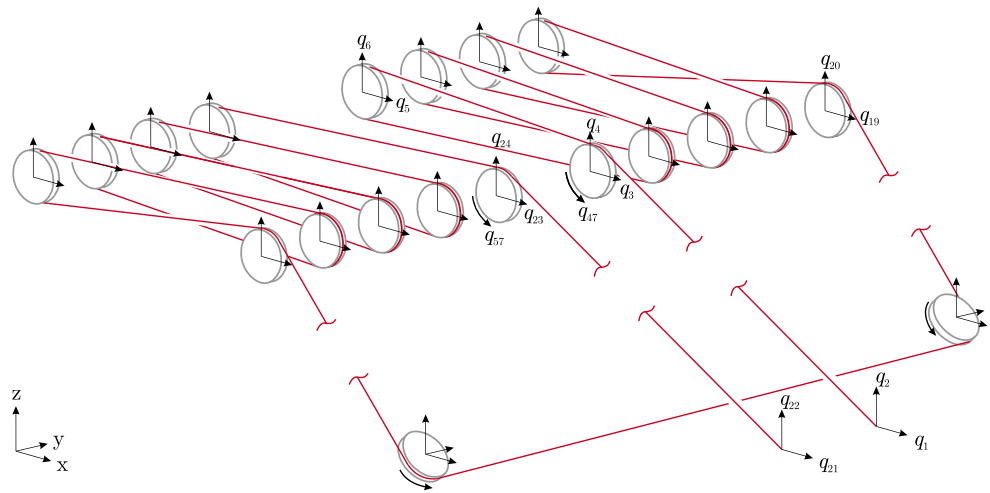
A special interest in the low-frequency dynamics arises as large vibration amplitudes on both booms occur during normal operation. Due to the operational vibrations, the service life of the load-carrying steel structure is limited. The main excitation source are the fluctuating cutting forces acting on the bucket wheel. Extensive testing has been performed by the operator to identify the mode shapes of the superstructure, which contribute to the excited operational deflection shape. Measurements of both the forced vibration responses resulting from the random cutting forces, and the decaying free vibration after changing predefined displacement boundary conditions were carried out using accelerometers at crucial points of the superstructure. The identified normal mode shapes are summarised in Table 2.

It is expected that the detailed modelling of the cable system will improve the correlation of lower natural frequencies and corresponding mode shapes between measured data and a finite element model of the system, depicted in Fig. 5.

Fig. 6 shows one of two cable systems to be modelled. The whole assembly possesses a mechanical advantage of 16 and is symmetrical about a vertical plane. Each end of the hoist rope is attached to a base-mounted drum hoist, located at the rear part of the ballast boom. An overall number of 20 pulleys guide the wire rope: 8 of them being located on top of the first pylon, 2 deflect the cable on the ballast boom and 10 are mounted on top of the second pylon.

Every pulley defines one attachment point of the cable system to the finite element model of the excavator's superstructure (see Fig. 5). The finite element model has been set up using Ansys Mechanical. The supporting structures consist of linear beam elements [16]. Only the welded assembly of the rotary platform is modelled with quadratic shell elements. Interface nodes between the steel structure and the cable system are located at the pulley positions on both pylons and at the position of the hoisting winches on the ballast boom. A total of 46 nodal coordinates associated with these interface nodes need to be coupled via the cable system's stiffness matrix.

The excavator's operating principle justifies the use of linear stiffness matrices for the cable system: The purpose of the analysis is to represent the vibration behaviour of the excavator when the cutting forces act and excite the whole structure. Hoisting only takes place between two consecutive cuts, when the inclination of the bucket wheel boom has to be changed. During the actual excavation process the superstructure is rotated around its vertical axis, but the mining height remains constant. This defines the spatial configuration of the cable system's attachment points (as shown in Fig. 5) and therefore specifies the location of each pulley.

The pulleys divide the wire rope into 21 cable segments of fixed length l_s, whose individual stiffness may be calculated according to [2] as $k_s = EA/l_s$. Herein, A is the total metallic area of the cable and E its effective modulus of elasticity at the current operating tension. Using Eq. (6) the potential energy of the cable system can be derived, allowing to calculate the yet unreduced stiffness matrix including the cable passages due to the pulley rotations. After applying the reduction scheme presented in Sect. 2 a coupling stiffness matrix relating all interface coordinates of the finite element model is obtained. This procedure can be automated using available symbolic math environments. Assembling the finite element model and the cable system's reduced stiffness matrix leads to the natural frequencies summarized in Table 2.

Due to the varying operating conditions and especially because of the changing conveying mass, the natural frequencies of the excavator are subject to continuous fluctuation. Table 2 hence only contains frequency ranges of the measured system responses and no distinction between
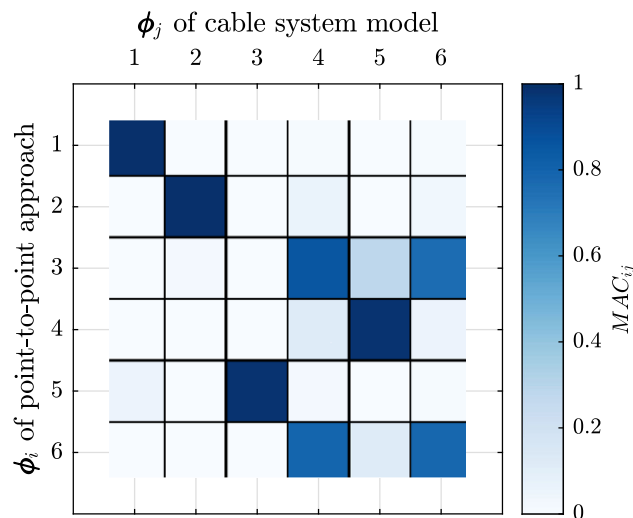
Fig. 7 Comparison of mode shapes using the Modal Assurance Criterion

damped and undamped frequencies is made. It is hereby demonstrated that the finite element model with a kinematically correct cable system correctly reproduces the real system's dynamic behaviour in terms of natural frequencies. In contrast, a point-to-point coupling of the attachment points overestimates the stiffness, leading to significantly increased natural frequencies.

Moreover, the mode shapes also differ. A common measure of consistency between two modal vectors is the Modal Assurance Criterion (MAC) [17]. In Fig. 7 the MAC-Matrix of the first six modal vectors of both discussed modelling approaches is depicted. High MAC-values on the main diagonal of the matrix denote a similarity between both models for the first two modes. Furthermore, the graphic proofs the interchange of normal modes, already seen in Table 2: e.g. mode number 3 of the cable system model corresponds to mode 5 of the point-to-point modelling approach. Considerable differences are revealed between the torsional mode shapes. A torsional deflection of the bucket wheel boom is directly related to a torsional deflection of the first pylon due to the guy ropes. As the point-to-point coupling approach neglects any balancing of cable tensions, a strong coupling between both pylons occurs, finally resulting in a deflection of the ballast boom. On the contrary, the cable system model allows angular misalignment of the pulley axes on both pylons, leading to a realistic system behaviour.

The presented simulation model of the excavator's elastic superstructure forms the basis for developing an active vibration control strategy in future work, using the inverter fed drives of the bucket wheel and the rotary platform as actuators.

5 Conclusion

The present article addresses a general method for integrating the flexible behaviour of pre-stressed cable-pulley systems into holistic numerical simulation models. First, a stiffness matrix of the cable-pulley assembly is calculated according to a strictly formal procedure based on the potential energy of all cable segments. The resulting stiffness matrix couples both deflections of the interface points (between the cable system and the attached structure) and additional coordinates of the pulley rotations, which are necessary to describe the kinematics of the mechanism. In order to avoid the necessity to extend the problem size of the holistic simulation model due to these additional rotational coordinates, a reduction scheme is used. Thus, the coupling between the displacement coordinates of all attachment points takes into account the cable passages, without explicitly introducing the respective degrees of freedom.

The approach is then applied to a simple block and tackle. A validation by means of a non-linear finite element model has been performed. Finally, the method is used to model an intricate hoisting cable system of a large-scale excavator. Due to the detailed cable system model a good agreement between measured vibration behaviour and simulation results is achieved. The cable system influences the natural frequencies of the superstructure. This leads to the general conclusion that the stiffnesses of large-scale steel structures and attached cable mechanisms can be of similar magnitude, which justifies an in-depth modelling. Furthermore, the kinematics of assemblies comprising of cable segments and pulleys influence the mode shapes of the whole system, as well as the load distribution between all interface points.

References

1. VDI 2358 (2012) Wire ropes for materials-handling equipment
2. Feyrer K (2007) Wire ropes: tension, endurance, reliability. Springer, Berlin, Heidelberg, New York

3. Costello GA (1997) Theory of wire rope. Springer, Berlin, Heidelberg, New York https://doi.org/10.1007/978-1-4612-1970-5
4. Winget J, Huston R (1976) Cable dynamics – a finite segment approach. Comput Struct 6(6):475–480. https://doi.org/10.1016/0045-7949(76)90042-0
5. Kamman J, Huston R (2001) Multibody dynamics modeling of variable length cable systems. Multibody Syst Dyn 5(3):211–221. https://doi.org/10.1023/A:1011489801339
6. Ozdemir H (1979) A finite element approach for cable problems. Int J Solids Struct 15(5):427–437. https://doi.org/10.1016/0020-7683(79)90063-5
7. Fried I (1982) Large deformation static and dynamic finite element analysis of extensible cables. Comput Struct 15(3):315–319. https://doi.org/10.1016/0045-7949(82)90022-0
8. Gosling P, Korban E (2001) A bendable finite element for the analysis of flexible cable structures. Finite Elem Anal Des 38(1):45–63. https://doi.org/10.1016/S0168-874X(01)00049-X
9. Bulín R, Hajžman M, Polach P (2017) Nonlinear dynamics of a cable-pulley system using the absolute nodal coordinate formulation. Mech Res Commun 82:21–28. https://doi.org/10.1016/j.mechrescom.2017.01.001
10. Aufaure M (1993) A finite element of cable passing through a pulley. Comput Struct 46(5):807–812. https://doi.org/10.1016/0045-7949(93)90143-2
11. Ju F, Choo Y (2005) Super element approach to cable passing through multiple pulleys. Int J Solids Struct 42:3533–3547. https://doi.org/10.1016/j.ijsolstr.2004.10.014
12. García-Fernández I, Pla-Castells M, Martínez-Durá J (2008) Elevation cable modeling for interactive simulation of cranes. In: Gross M, James D (eds) Eurographics symposium on computer animation
13. Coulibaly J, Chanut MA, Lambert S, Nicot F (2018) Sliding cable modeling: an attempt at a unified formulation. Int J Solids Struct 130-131:1–10. https://doi.org/10.1016/j.ijsolstr.2017.10.025
14. Geradin M, Rixen D (2015) Mechanical vibrations, 3rd edn. John Wiley & Sons Inc., Hoboken
15. Guyan R (1965) Reduction of stiffness and mass matrices. AIAA J 3(2):380. https://doi.org/10.2514/3.2874
16. Schulz C (2014) Ganzheitliche Systemanalyse von Schaufelradantrieben. Ph.D. thesis, TU Dresden, IMM
17. Allemang R (2003) The modal assurance criterion – twenty years of use and abuse. Sound Vib 37(8):14–21